

# The nature of marbled Terra Sigillata slips: a combined $\mu$ XRF and $\mu$ XRD investigation

Y. Leon<sup>a,b</sup>, Ph. Sciau<sup>a,b</sup>, Ph. Goudeau<sup>c</sup>, N. Tamura<sup>d</sup>, S. Webb<sup>e</sup>, A. Mehta<sup>e</sup>

<sup>a</sup> CNRS, CEMES, BP 94347, 29 rue Jeanne Marvig, 31055 Toulouse, France

<sup>b</sup> Université de Toulouse, UPS, INSA, CEMES, 31055 Toulouse, France

<sup>c</sup> PhyMat, Université de Poitiers, CNRS, SP2MI, 86962 Futuroscope Chasseneuil, France

<sup>d</sup> ALS, LBNL, 1 Cyclotron Road, Berkeley, CA 94720, USA e SSRL, SLAC, University Stanford, 2575 Sand Hill Rd., Menlo Park, CA 94025, USA

Y. Leon: tel: +33 5 62 25 78 24, Fax: +33 5 62 25 79 99, e-mail: [Yoanna.Leon@cemes.fr](mailto:Yoanna.Leon@cemes.fr)

Ph. Sciau: tel: +33 5 62 25 78 50, Fax: +33 5 62 25 79 99, e-mail: [Philippe.Sciau@cemes.fr](mailto:Philippe.Sciau@cemes.fr)

Ph. Goudeau: tel : +33 5 49 49 67 26, Fax: +33 5 49 49 66 92, email: [pgoudeau@univ-poitiers.fr](mailto:pgoudeau@univ-poitiers.fr)

N. Tamura: tel : +1 510 486 6189, Fax: + 1 510 486 7696, email: [ntamura@lbl.gov](mailto:ntamura@lbl.gov)

A. Mehta: tel: +1 650 926 4791, Fax: +1650 926 4100, email: [mehta@slac.stanford.edu](mailto:mehta@slac.stanford.edu)

PACS numbers: 78.70.En (X-ray emission spectra and fluorescence), 61.05.cp (X-ray diffraction), 07.85.Qe (synchrotron radiation instrumentation), 68.55.Nq (Composition and phase identification).

Corresponding author: Philippe Sciau ([Philippe.Sciau@cemes.fr](mailto:Philippe.Sciau@cemes.fr))

**ABSTRACT:** In addition to the red terra sigillata production, the largest Gallic workshop (La Graufesenque) made a special type of terra sigillata, called “marbled” by the archeologists. Produced exclusively on this site, this pottery is characterized by a surface finish made of a mixture of yellow and red slips. Because the two slips are intimately mixed, it is difficult to obtain the precise composition of one of the two constituents without contamination by the other. In order to obtain very precise correlation at the appropriate scale between the color aspect and the element and mineralogical phase distributions in the slip, combined electron microprobe, x-ray micro spectroscopies and micro diffraction on cross sectional samples were performed. The aim is to discover how potters were able to produce this unique type of terra sigillata and especially this slip showing an intense yellow color. Results show that the yellow component of marbled sigillata was made from a titanium-rich clay preparation. The color is related to the formation of a pseudobrookite (TiFe<sub>2</sub>O<sub>5</sub>) phase in the yellow part of the slip, the main characteristics of that structure being considered nowadays as essential for the fabrication of stable yellow ceramic pigments. Its physical properties such as high refractive indices and a melting point higher than that of most silicates widely used as ceramic colorants are indeed determinant for this kind of applications. Finally, the red parts have a similar composition (elementary and mineralogical) to the one of standard red slip.

## 1 Introduction

Terra sigillata is certainly the most famous fine ware of the Roman period showing cast decors achieved with the help of stamps (sigilla). Massively produced in standardized shapes and widely

distributed, sigillata production can be traced back as the industrial activity of a few specialized workshops [1]. In the literature, the terra sigillata is also often identified as a ceramic with red high-gloss coating, obtained through the vitrification of an iron oxide-rich clay preparation under oxidizing conditions. Even though a great majority of sigillata ceramics has a red coating, the color alone cannot be considered as a defining characteristic. For example, during the first century AD, in one of the Gallic workshops, terra sigillata were indeed made with another type of color for coating.

The yellow color in terra sigillata slips was first described in the early publications on the large Gallic workshop of La Graufesenque (Millau, France) and identified as a speciality of this workshop [2] [3] [4]. From the beginning, this singular yellow high-gloss coating with red veins (see Figure 1), often called “marbled” because of this marble aspect, has intrigued the archaeologists. Considered at first as an epiphenomenon taking place for a short period, recent investigations seem to indicate that the production of this type of coatings started around 30 AD and continued until the end of the first century i.e during a great part of the massive production period of La Graufesenque's workshop [5]. Although marbled sigillata represents only a few percent of La Graufesenque productions, several officine were implicated in its fabrication. The distribution of the marbled sigillata was as wide as that of standard red sigillata, but with a higher representation in the Mediterranean basin.

Marbled sigillata coating results from firing a vessel dipped into mixture of two different liquid slips intimately mixed. The red part of the fired slip gets its color from the hematite and appears to be very similar to the slip on a standard red sigillata vessel [6]. However, besides one analysis revealing a high titanium content [7], very little is known about the yellow component of the marbled slip. The major set back in obtaining a fuller analysis and deeper understanding of the yellow parts of the marbled slip arises from the intimate mixing of the red and the yellow slips in the coating and most conventional analysis of the yellow parts of the slip are contaminated by the red part. The aim of this study is therefore to use micron size electron and x-ray beams to easily separate the two components of the slip and determine the nature of yet very poorly understood yellow component. For that purpose, we used electron microprobe to obtain the global elemental composition of the yellow slip and then, combined optical microscopy, x-ray micro spectroscopy and micro diffraction to correlated the variation in the color in the slip with mineralogical phases and element distribution.

## **2 Experimental**

Five shards of marbled sigillata (noted TSGM-A, -B, -C, -D and -E) were selected by Alain Vernhet who has managed the excavations of La Graufesenque's site for many years. The samples originate from different zones of excavations dated between 40 AD and 60 AD.

The shards were cut with a diamond saw to obtain fresh cross-sections, which were mounted in epoxy and then mechanically polished. Elementary analyses were performed on the polished surface using the CAMECA SX50 microprobe of the Laboratory of the Mechanisms and Transfers in Geology (LMTG) of the Paul Sabatier University (Toulouse). The operating conditions were: accelerating voltage of 15kV, beam current of 20nA and analyzed surface approximately  $2 \times 2 \mu\text{m}^2$ . Natural and synthetic minerals were used as standards, and particular attention being taken to avoid alkali metal migration [8].

In order to correlate the color to element and mineralogical phase distributions, a combination of x-ray microprobe and micro diffraction was performed on a polished cross section of the marbled slip, which was previously studied in an electron microprobe (Fig. 2).

We chose the delimited area of the TSGM-A shard shown in figure 1 for which the yellow part of the slip is the largest and the most homogeneous. There is a tremendous advantage in performing all the measurements, including the standard archaeological (such as optical microscopy, SEM, electron microprobe...) and synchrotron based micro x-ray diffraction ( $\mu$ XRD) and micro x-ray fluorescence ( $\mu$ XRF), as it makes correlation among them easy and transparent to combine them to obtain complementary information, but it does cause the experimental complication of performing x-ray measurements in reflection geometry. Further, to obtain the highest quality  $\mu$ XRD and  $\mu$ XRF measurements we decided to perform these measurements on two different beamlines, which were dedicated and optimized for them. Our experimental strategy, thus, involved transporting the same polished and mounted pottery shard between two continents and several different instruments, and therefore, imposed the challenge of locating the region of interest very quickly and precisely when moving the sample from one instrument to another instrument. For that purpose, Pt ( $10 \times 30 \mu\text{m}^2$ ) registration marks were deposited just outside the region of interest by crossbeam focused Ion beam equipped with gas injection system (Fig. 3) and all the measurements were done with reference to them.

The  $\mu$ XRF study was carried out on beamline 2.3 at the Stanford Synchrotron Radiation Lightsource -SSRL (Stanford, USA). This line is a multipurpose station used for  $\mu$ -XRF, chemical imaging, XANES/EXAFS, and also diffraction analysis but only in transmission and monochromatic mode. The typical x-ray beam size on the sample surface was  $2 \times 2.5 \mu\text{m}^2$  using Kirkpatrick–Baez focusing system. The excitation range energy was set to 2.4 -30 keV (covers actinide L edges and Ti K-edge), using a Si (111) double-crystal monochromator. At each  $5 \mu\text{m}$  step, fluorescence signals were collected using a high-purity Ge solid state detector with recording time of about 100 -300 msec (with the total scan time for sample between 20 min to 6 hr).

The micro scanning XRD measurements were carried out at beamline 12.3.2 of the Advanced Light Source (Berkeley, USA). The cross sectional sample, mounted on a XY piezoelectric stage can be successively step-scanned under polychromatic (5-25 keV) or monochromatic (8.75keV) beams [9]. Fluorescence signals as well as diffraction patterns were collected using respectively a VORTEX Si-drift detector and a MAR133 CCD camera (133 mm diameter active area) placed on radial translational stage. However, the beam line is dedicated for micro diffraction and not optimized for fluorescence measurements. We used the fluorescence measurements only to locate the Pt registrations marks. The powerfulness of the beam line is related to easy change between monochromatic and polychromatic modes keeping the focus point unchanged on the sample surface. For monochromatic studies, the typical x-ray beam size at the sample surface was about  $2 \times 4 \mu\text{m}^2$  and the step size used was  $2 \mu\text{m}$ . The x-ray incident angle was fixed at  $15^\circ$  whereas the angular swing position of the CCD camera was set to  $40^\circ$ . In this paper, the reported polychromatic beam results concern only the experiment calibration done using a silicon single crystal reference sample. A laser based set up was used for setting the sample surface at the goniometer center with an accuracy better than  $10 \mu\text{m}$ . All the diffraction Laue and powder diffraction patterns were analyzed using the XMAS software available at the beam line web site (<http://xraysweb.lbl.gov/microdif/>) for users.

### **3 Results and discussion**

#### **3.1 Evaluation of the elementary composition of yellow parts by electronic microprobe**

As the two slip colors are intimately mixed, the main difficulty was to cleanly separate one slip from the other and minimize cross-contamination between them. After preparation, the five cross-section specimens were carefully examined by optical microscopy and 7 areas of relatively homogeneous yellow color such as the one shown in figure 2 were selected for electron microprobe measurements. The first salient result of this study was the large compositional heterogeneity of the yellow component with strong fluctuations in composition of titanium, calcium and magnesium elements. Then, in order to fully quantify the local variation in composition, a great number of spot measurements were made in each zone. The few measurements close to the red slip were not considered for the average calculation. The results from the spot measurements are given in table 1. In Table 2 the average composition of a standard red slip is given for comparison [10]. These new results are consistent with the published one [7]. The yellow slip distinguishes itself from the red slip by a strong increase of titanium and magnesium concentration, no significant difference in aluminum, potassium and silicon concentration, and a proportional decrease of iron content. The strongest heterogeneity at a local scale is in iron and titanium concentration, resulting in large standard deviation (given in brackets), but the silicon concentration appears to be fairly homogeneous. Even with the use of small spot size for measurements, we cannot exclude the possibility that the analyzed zones are completely exempt of red component and some of the iron content in the yellow slip and perhaps even the origin of the compositional variations lies in this red slip contamination. Nevertheless, the results obtained for the seven analyzed areas appear to be compositionally similar suggesting that we were fairly successful excluding majority of red component from our measurements. Because of the fairly close average Ti and Fe composition of yellow slip from the seven different areas, but large standard deviation in them in the average from each area suggests perhaps that the yellow slips are, indeed, inherently heterogeneous at a very local scale.

#### **3.2 Synchrotron $\mu$ XRF and $\mu$ XRD studies**

Figure 3 shows the x-ray fluorescence maps obtained at SSRL for the TSGM-A sample. The slip, which has a much higher potassium concentration and much lower calcium concentration, easily differentiates itself from the body (paste) of the ceramic in the Ca and K fluorescence maps. The two color components of the slip are also easily identified, by a higher iron concentration in the red part, and higher titanium concentration in the yellow part, as is in agreement with the electron microprobe measurements (Table 2). To precisely study the boundary between the two different color slips, a finer, higher resolution scan ( $2 \times 2 \mu\text{m}^2$ ) was performed over a region where yellow slip covers a thin layer of the red slip, of about  $10 \mu\text{m}$  thickness (Fig. 5a). The yellow part is quite large and still found to be homogeneous in composition. Additional XRF maps were collected at 3 different energies (7.122, 7.134 and 7.138 keV) over the Fe K-edge to generate Fe<sup>2+</sup> and Fe<sup>3+</sup> maps. The maps were generated from difference in Fe<sup>2+</sup> and Fe<sup>3+</sup> absorbances at these energies, previously determined from XANES spectra on reference compounds. All the iron in the potter sherd, in both slip and the body region was found to be Fe<sup>3+</sup> (Fe valence maps are not shown here,

but shown in ref. [11], where difference in valence was found). Full Fe K-edge XANES spectra were recorded at several selected spots in the paste, yellow and red layers and compared to a database of iron mineral references. Spectra recorded in paste and red layer are similar to the one of hematite while those in the yellow part were found to be different, but not conclusively identified (but subsequently identified based on microdiffraction measurements described below).

MicroXRD were performed at the ALS on the selected area of figure 5(a). These regions precisely located thanks to Pt marks, which are easily identified by fast  $\mu$ XRF scans at the beam line. The beamline allows both monochromatic and polychromatic diffraction configurations. Despite the fact that the two modes were used, only the results obtained with monochromatic x-ray beams are given in this paper. In fact, most of the crystals in the slips have a size much smaller than the beam size (about 1 micron). In that case, only the monochromatic mode allows for reliably indexable diffraction data. The white beam was used for the study of crystallites whose size was greater than the beam size (as for these crystallites, monochromatic conditions did not give indexable diffraction patterns.) In the case of slips, this population of large crystallites is small and they are mainly quartz crystals and of not that much interest in this investigation. Nevertheless, interesting complementary information such as crystallite size, orientation and strains can be extracted from the Laue diagrams from these large crystallites collected with white x-ray beams. These results will be presented in a forthcoming paper detailing white beam applications to different type of antic slips.

Characteristic diffraction diagram of each layer is presented in figure 4. These diagrams were obtained by integration along rings of 2D patterns. The two constituents of the slip are very different regarding mineral composition. The red part has the exact composition of the standard red slip [12] with hematite and corundum as the main phases while the dominant phase in the yellow part is a pseudobrookite ( $\text{TiFe}_2\text{O}_5$ ). The yellow component also contains spinel, corundum and, in less proportion, a feldspar of anorthite type. The paste has the compositional characteristics of terra sigillata from La Graufesenque i.e. a significant amount of anorthite and a quasi absence of pyroxene [13]. Quartz contribution was also identified in all diffraction diagrams with weak intensity diffraction peaks. However, a careful inspection of the 2D diffraction patterns shows that quartz crystals give isolated diffraction peaks indicating large grain size ( $> 1$  micron). As mentioned before, monochromatic x-ray beam with micrometer size is not suitable for the study of the quartz phase. On the other hand, the 2D diffraction patterns reveal that spinel and corundum phases give continuous diffraction rings, typical of phases with nanometric sizes while the intensity of diffraction rings of hematite and pseudobrookite show discontinuities (spotty rings) indicating larger grain size, in the ranging from several hundred nanometers to about one micron.

Results of the scan made on the area investigated by  $\mu$ XRF are given in figure 5. The phase maps were obtained by integrating different peaks in each phase at every point of the X-Y scan. The area showing high concentration in pseudobrookite and spinel phases corresponds to the yellow part identified as titanium rich by XRF. The spatial repartition of pseudobrookite and spinel shows a strong variation indicating the origin of the heterogeneities in the crystalline composition of the yellow part. The red component is less well resolved; this is due to its small width (8-10  $\mu\text{m}$ ) compared to the beam size used (2  $\mu\text{m}$  in the direction normal to the interface). Moreover, the x-ray beam penetration must be also considered (about 20  $\mu\text{m}$  at 8 keV) as well as the interface roughness along the beam direction to estimate the spatial resolution. Unfortunately, under these conditions it is difficult to clearly separate the contributions from the two components at interfaces. Nevertheless, a higher concentration for hematite phase is observed in the region located between

the paste and the yellow surface layer. This result is clearly visible in figure 6 where linear scans across the slip have been done for all different phases. This interlayer, which is related to the red layer, is also characterized by the absence of anorthite (paste) and pseudobrookite (yellow layer) phases. Corundum is clearly distributed in both the two slip layers, but has a higher concentration in the yellow layers. The situation is more ambiguous for the spinel, which seems to present in the red part close to the yellow part. However our resolution is too poor to investigate, for instance, whether this accumulation at the interface is driven by diffusion phenomenon between the two slips.

#### **4 Concluding remarks**

Our results confirm that the red part of the marbled slip has the same origin as the standard red slip used in the La Graufesenque's workshop. The correlation between elemental and mineral compositions allowed us to determine the crystallographic nature of the yellow component. It contains small crystals of pseudobrookite, a Ti-rich phase, which is certainly responsible for the yellow color. It is intriguing that just over the few years, pseudobrookite has again been considered for obtaining yellow pigments used in modern ceramic decoration [14]. Indeed, this phase is able to confer a high stability to the yellow pigment, which is of critical importance to the decorative ceramic industry. However, the relation between the existence of a phase and the color stability of the pigment is complex since the color depends on the firing temperature and the ceramic matrix composition containing this phase. In a few recent studies on use of pseudobrookite for yellow pigmentation on decorative ceramic [15], the resulting coloration is rather brown, but cause of the brown coloration is not fully understood. It would be interesting to expand these studies and employ techniques described here to study pigmentation layers at microscopic scale. Investigation of the pigment layer at this scale will allow precise determination of the composition of the matrix and morphology and relationship pseudobrookite crystals to the surrounding matrix. It will be particularly important to determine the Fe/Ti ratio, which will certainly play a major role in the overall color. In addition, the chemical composition of the spinel crystals could have a significant influence on the global resultant color.

Considering the high level of titanium content in the yellow areas of the marbled slips, Maurice Picon [7] started searching for their origin among the local volcanic Ti-rich clays. After exploring various sites, the best concordances have been found with some clays of the submarine formation "des Vignes" which are also the only ones rich in potassium. The hypothesis that these clays were the origin of the La Graufesenque yellow seems quite plausible in view of the results presented here. The absence of Fe<sup>2+</sup> iron, good vitrification of slip, mineral composition of the paste (body) and of the red part show that these sigillata were fired with the same protocol used for standard sigillata production (i.e., fired under oxidizing condition around 1050°C) [13] [16].

#### **Acknowledgements**

The authors thank A. Vernhet and M. Kunz for artefact specimens and for assistance during experiments at ALS beamline 12.3.2, respectively. This work was supported by the Conseil Régional de Midi-Pyrénées under contract No. 06001527, a France–Stanford Center grant for the 2006–2007 academic years and the Director, Office of Science, Office of Basic Energy Sciences, of the U.S. Department of Energy who is operating ALS and SSRL under Contracts No. DE-

AC02-05CH11231 and DE-AC02-76-SFO0515, respectively. The upgrade of the ALS beamline 12.3.2 was enabled through the NSF grant # 0416243 obtained through the Iowa State University.

## **REFERENCES**

- 1 M. Madrid Fernández, J. Buxeda i Garrigós, in 5th European Meeting on Ancient Ceramics, edited by V. Kilikoglou, A. Hein, and Y. Maniatis (Archaeopress, Athens, 1999), pp. 287.
- 2 J. Déchelette, *Revue des Etudes Anciennes* 5, 1 (1903).
- 3 F. Oswald, T.-D. Pryce, *An introduction to the study of terra sigillata*. (London, 1920).
- 4 F. Hermet, *La Graufesenque, Condatomogos, vases sigillés, graffites*. (Paris, 1934).
- 5 M. Genin, in *La Graufesenque (Millau, Aveyron); Sigillées lisses et autres productions*, edited by M. Genin (Bordeaux, 2007), Vol. II, pp. 155.
- 6 P. Sciau, S. Relaix, C. Roucau, Y. Kihn, *J. Am. Ceram. Soc.* 89, 1053 (2006).
- 7 M. Picon, *Rev. Archéo.* 21, 86 (1997).
- 8 J. G. Spray, D. A. Rae, *Canadian Mineralogist* 33, 323 (1995).
- 9 N. Tamura, R. S. Celestre, A. A. MacDowell, H. A. Padmore, R. Spolenak, B. C. Valek, N. M. Chang, A. Manceau, J. R. Patel, *Rev. Sci. Instrum.* 73, 1369 (2002).
- 10 P. Sciau, C. Dejoie, S. Relaix, D. Parseval, in *La Graufesenque (Millau, Aveyron); Sigillées lisses et autres productions*, edited by M. Genin (Bordeaux, 2007), Vol. II, pp. 23.
- 11 C. Mirguet, P. Sciau, P. Goudeau, A. Metha, P. Pianetta, Z. Liu, N. Tamura, *Adv. X-Ray Anal.* 51, 242 (2008).
- 12 P. Sciau, P. Goudeau, N. Tamura, E. Dooryhee, *Appl. Phys. A* 83, 219 (2006).
- 13 P. Sciau, M. Werwerft, A. Vernhet, C. Bemont, *Rev. Archéo.* 16, 89 (1992).
- 14 M. Dondi, F. Matteucci, G. Cruciani, G. Gasparotto, *Solid State Sciences* 9, 362 (2007).
- 15 M. Dondi, G. Cruciani, E. Balboni, G. Guarini, C. Zanelli, *Dyes and Pigments* 77, 608 (2008).
- 16 P. Sciau, S. Relaix, C. Mirguet, A. M. T. Bell, R. L. Jones, E. Pantos, *Appl. Phys. A* 90, 61 (2008).

## Tables

Shard	Na <sub>2</sub> O	MgO	Al <sub>2</sub> O <sub>3</sub>	SiO <sub>2</sub>	P <sub>2</sub> O <sub>5</sub>	K <sub>2</sub> O	CaO	TiO <sub>2</sub>	MnO	Fe <sub>2</sub> O <sub>3</sub>	BaO	total
<b>TSGMA-1</b> <b>(34)</b>	0.08 (0.04)	2.19 (1.21)	23.30 (4.43)	55.53 (9.94)	0.09 (0.06)	7.29 (1.21)	1.64 (0.99)	4.18 (7.31)	0.03 (0.03)	5.08 (4.18)	0.14 (0.12)	99.47 (1.52)
<b>TSGMA-2</b> <b>(30)</b>	0.08 (0.05)	2.18 (0.88)	23.09 (4.35)	56.11 (7.20)	0.08 (0.07)	7.86 (1.23)	2.22 (1.28)	3.17 (2.42)	0.04 (0.03)	4.48 (2.20)	0.17 (0.11)	99.48 (1.72)
<b>TSGMB</b> <b>(25)</b>	0.05 (0.04)	2.54 (0.82)	21.01 (2.39)	56.16 (3.59)	0.15 (0.05)	7.92 (0.62)	2.24 (1.02)	3.60 (1.70)	0.05 (0.04)	4.67 (1.98)	0.14 (0.15)	98.53 (0.95)
<b>TSGMC-1</b> <b>(28)</b>	0.05 (0.04)	2.66 (1.11)	22.48 (3.58)	56.54 (6.01)	0.11 (0.05)	7.67 (0.70)	2.24 (1.23)	3.40 (2.13)	0.03 (0.04)	4.22 (1.85)	0.14 (0.11)	99.54 (1.02)
<b>TSGMC-2</b> <b>(37)</b>	0.05 (0.03)	2.92 (0.87)	22.72 (1.60)	56.41 (3.35)	0.09 (0.05)	7.63 (0.58)	2.07 (0.97)	3.21 (2.00)	0.05 (0.04)	4.47 (1.73)	0.14 (0.04)	99.75 (1.06)
<b>TSGMD</b> <b>(54)</b>	0.05 (0.03)	2.42 (0.83)	21.01 (2.54)	57.18 (5.44)	0.11 (0.06)	9.35 (0.74)	1.69 (0.46)	3.61 (2.58)	0.03 (0.03)	4.49 (2.03)	0.14 (0.14)	100.08 (1.30)
<b>TSGME</b> <b>(26)</b>	0.06 (0.05)	2.46 (0.43)	20.73 (1.42)	56.62 (3.59)	0.09 (0.04)	7.65 (0.45)	1.61 (0.47)	3.66 (2.11)	0.04 (0.04)	4.62 (1.87)	0.17 (0.14)	97.72 (0.96)

Table 1: Chemical composition of seven areas from five marbled sigillata shards. The number of measurements and the standard deviations are given in bracket.

Slip	Na <sub>2</sub> O	MgO	Al <sub>2</sub> O <sub>3</sub>	SiO <sub>2</sub>	P <sub>2</sub> O <sub>5</sub>	K <sub>2</sub> O	CaO	TiO <sub>2</sub>	MnO	Fe <sub>2</sub> O <sub>3</sub>	BaO
<b>Yellow</b> <b>(7)</b>	0.06 (0.02)	2.50 (0.26)	22.24 (1.09)	56.81 (0.51)	0.10 (0.03)	7.97 (0.67)	1.97 (0.30)	3.58 (0.34)	0.04 (0.01)	4.60 (0.26)	0.15 (0.02)
<b>Red</b> <b>standard</b> <b>(38)</b>	0.07 (0.02)	0.89 (0.15)	23.27 (2.44)	55.70 (2.30)	0.15 (0.03)	8.19 (0.76)	1.24 (0.27)	0.72 (0.10)	0.05 (0.01)	9.62 (0.82)	0.08 (0.02)

Table 2: Mean chemical composition of the yellow constituent compared to mean chemical composition of the red standard slip obtained from 38 shards (ref 10). The standard deviations are given in brackets.



**Figures**

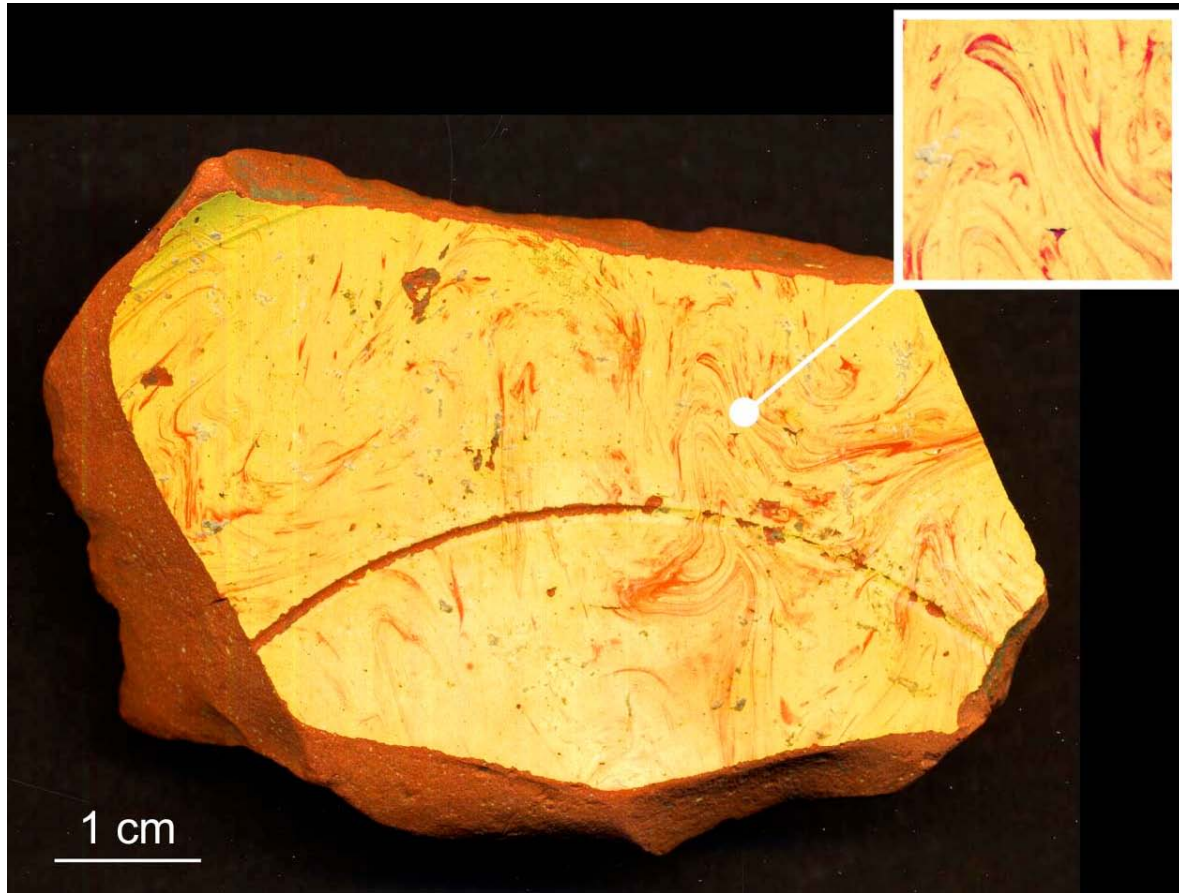


Figure 1 (color online) Fragment of marbled sigillata from La Graufesenque. The inset dimension are 1 x 1 cm<sup>2</sup>.

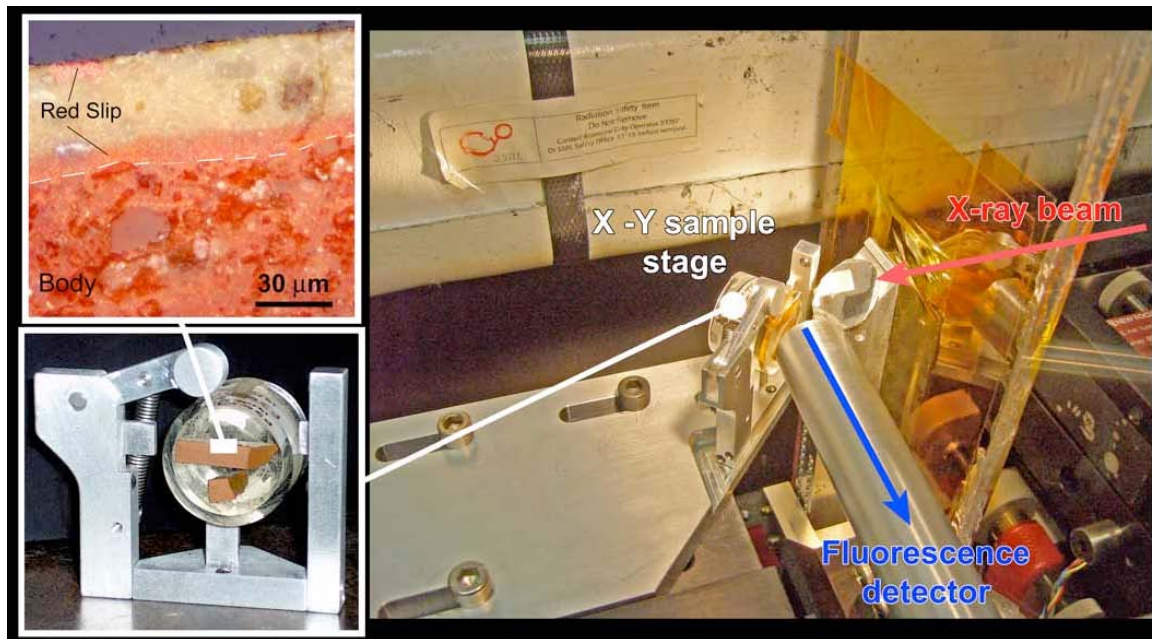


Figure 2 (color online) Electron microprobe sample at 2.3 SSRL (USA) beam line with a detail of cross section slip observed by optical microscopy (x400).

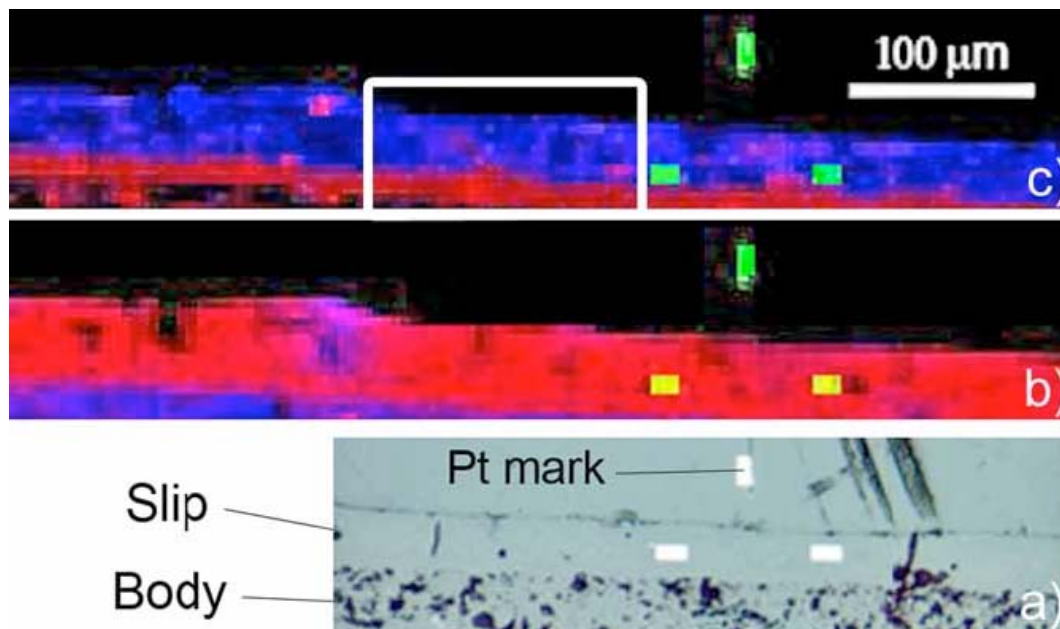


Figure 3 (color online) TSGM-A marbled sigillata cross section. a) optical microscopy observation of Pt mark (3 white rectangles),  $\mu$ XRF maps ( $5 \times 5 \mu\text{m}^2$  X-Y step scan size,  $2 \times 2.5 \mu\text{m}^2$  beam size at the sample surface), b) Ca blue, K red, Pt green and, c) Ti blue, Fe red, Pt green.

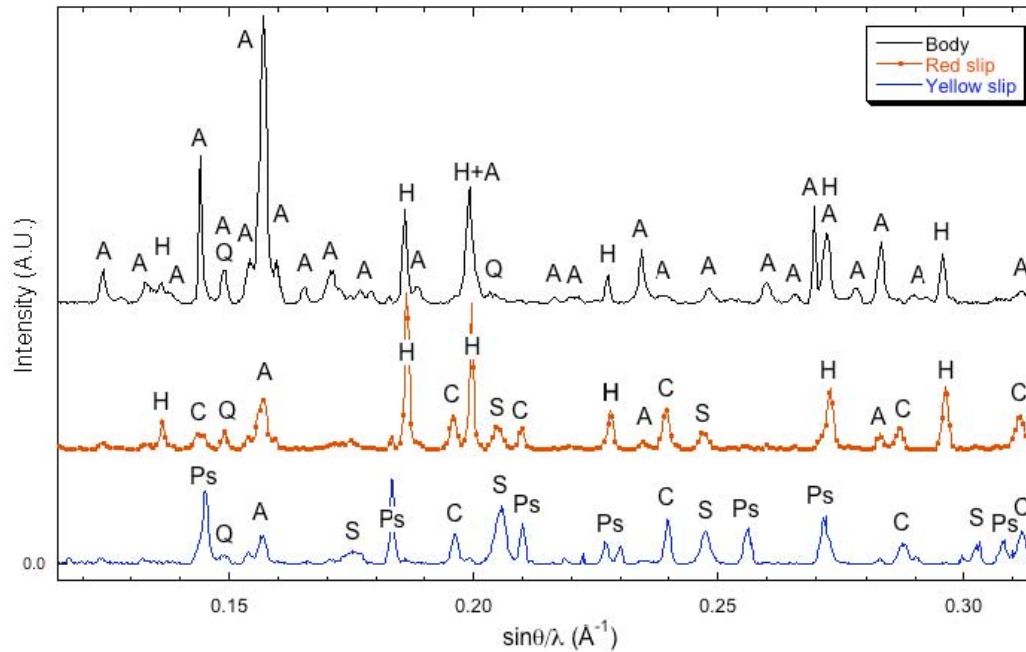
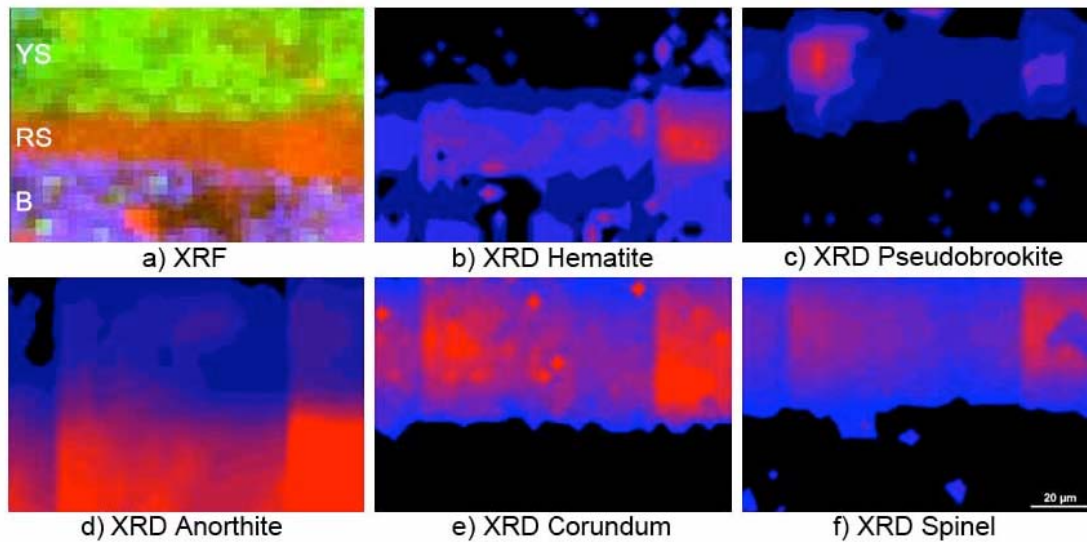


Figure 4 (color online) Characteristic diffraction diagrams of each parts obtained after  $\chi$  angular integration (i.e. along the powder diffraction rings) of 2D monochromatic diffraction patterns. A: anorthite, H: hematite, Q: quartz, C: corundum, Ps: pseudobrookite, S: spinel Figure 5 (color online) a) XRF map (X-Y step scan size: beam size at the sample surface:  $2 \times 2 \mu\text{m}^2$ ,  $2 \times 2.5 \mu\text{m}^2$ ) of delimited area shown on Figure 3 measured at SSRL and corresponding mineralogical maps obtained by integrating the intensity over a given diffraction ring (d-spacing in nm) recorded at ALS ( $2 \times 2 \mu\text{m}^2$  pixels,  $2 \times 3 \mu\text{m}^2$  beam): (b) hematite at  $d=0.270$ , (c) pseudobrookite at  $d=0.275$ , (d) anorthite at  $d=0.320$ , (e) corundum at  $d=0.209$  and (f) spinel at  $d=0.244$ .



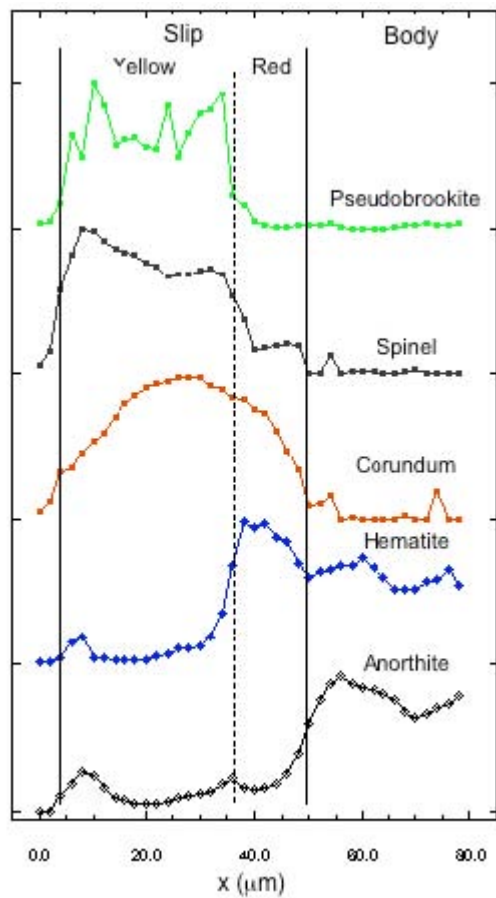


Figure 6 (color online) Linear micro scanning XRD on TSGM-A cross section sample showing the phase distribution in the slip and the paste (body).